Analysis of the transverse momentum collective motion in heavy-ion collisions below 100 MeV/nucleon

V. de la Mota,[2] F. Sebille,[1] M. Farine,[1] B. Remaud,[1] and P. Schuck[3]
[1]*Laboratoire de Physique Nucléaire, Institut National de Physique Nucléaire et de Physique des Particules, Centre National de la Recherche Scientifique, Université de Nantes, 2 rue de la Houssinière, 44072 Nantes, CEDEX 03, France*
[2]*Grand Accélerateur National d'Ions Lourds, Boîte Postale 5027, 14021 Caen, CEDEX, France*
[3]*Institut des Sciences Nucléaires, F-38026 Grenoble, CEDEX, France*
(Received 23 December 1991)

A theoretical analysis of collective momentum transfer is performed in heavy-ion reactions below 100 MeV/nucleon in the Landau-Vlasov approach. The nucleon-nucleon cross section, atomic mass, compressibility, and effective mass dependences are analyzed. The simulation of detector acceptances and of finite number of detected particles are discussed. In connection with recent experiments, theoretical results and experimental data are confronted taking into account the experimental constraints. Finite range forces of the Gogny type connected with different nuclear matter incompressibilities are used and the ensuing sensitivity of the flow is studied. The question whether the flow provides information on out-of-equilibrium matter properties is investigated.

PACS number(s): 25.70.Gh, 24.10.−i

I. INTRODUCTION

The search for information on the nuclear equation of state (EOS) and on the rate of two-body collisions from heavy-ion reactions remains one of the principal goals of nuclear physics. With this purpose many theoretical and experimental investigations are currently performed in a wide range of beam energies. A considerable effort has been devoted [1] to the study of the nuclear collective flow in high energy reactions, mostly above 200 MeV/nucleon. In this range of energies, all theoretical models find a net dependence of the calculated flow on the incompressibility modulus of nuclear matter, K_∞, when local effective forces are used. However, when more realistic momentum-dependent forces are implemented, the determination of K_∞ becomes much more delicate. In this high energy regime another difficulty arises, since the two-body collisions contribute predominantly to the formation of sideward nucleon flow, and therefore the sensitivity of the flow to the EOS parameters is very weak [2].

In this respect we shall consider here heavy-ion collisions at lower energies (between 50 and 150 MeV/nucleon), where the collective flow is expected to lessen and even to change sign [3]. The absolute value of the collective transverse motion is much smaller than at higher energies, but this drawback is to a large extent made up by other features. For instance, heat production is less important than compression [4], and then we can expect a greater sensitivity to the cold EOS than in reactions at higher energies. Furthermore, the energy of vanishing flow (EVF) can be measured more precisely than the flow itself, since it is less affected by experimental biases.

This paper presents the results of a theoretical analysis of collective momentum transfer. The calculations are made with the Landau-Vlasov code [5], which has been already used to study the flow at higher energies [6]. Our objective is to complete a line of investigation initiated in a previous work [2], concentrating on the collective flow properties in the vicinity of beam energies close to the EVF. Two lines of investigation will be followed: (i) the flow analysis which focuses on the mean transverse momentum at midrapidity, (ii) the transverse momentum analysis [7], where the average momentum in the reaction plane is studied as a function of the rapidity.

More and more experiments are performed with 4π detectors, and detailed confrontations with experimental data are now possible [8] even at low beam energies. The reaction products may have relatively low velocities in the laboratory frame, the measures of which are then very sensitive to the acceptance of the detectors. On the other hand, the finite number of constituents and the missing momentum carried by the undetected fragments lead to uncertainties in the determination of the reaction plane. We shall discuss how the bare theoretical results can be treated in order to simulate these experimental biases.

This work is organized as follows: In Sec. II a brief survey of the theoretical model is given. In Sec. III comparisons with experimental measures are performed with a special analysis in the energy range where the flow vanishes. In Sec. IV the informations which can be extracted from experiments below 100 MeV/nucleon are discussed; in particular, the sensitivity of transverse collective modes to the parameters of the effective nuclear interaction is analyzed. We present our conclusions in Sec. V.

II. THEORETICAL BACKGROUND

Our dynamical description of a heavy-ion collision is based on the Landau-Vlasov equation for the one-body

distribution function $f(\mathbf{r},\mathbf{p};t)$:

$$\frac{\partial f}{\partial t}+\{f,H\}=I_{\text{coll}}(f)\ . \tag{2.1}$$

Here the symbol $\{\ ,\ \}$ stands for the Poisson bracket, H is the average mean field, and I_{coll} is the Uehling-Uhlenbeck collision term. A variety of methods have been used to solve Eq. (2.1), their validity depending on the energy range of interest. Our procedure, usually referred to as the Landau-Vlasov model [5], is based on the projection of one-body phase space onto a continuous basis of coherent states g:

$$f(\mathbf{r},\mathbf{p})=W(\mathbf{r},\mathbf{p})*g(\mathbf{r},\mathbf{p})\ . \tag{2.2}$$

These states are chosen as normalized Gaussians with fixed widths, the centers of which move in the self-consistent field, following Ehrenfest-type equations and suffering hard stochastic scattering among them. The weight function W gives the occupation probability of the coherent state trajectories, and it is usually taken at the Thomas-Fermi limit for ground states (for more details, see Ref. [5]).

To study EOS effects on the nuclear dynamics, the average field has often been calculated with a local Skyrme-type force (Zamick force), which in terms of the local density $\rho(\mathbf{r})$ reads

$$V_{\text{HF}}(\mathbf{r})=a\frac{\rho(\mathbf{r})}{\rho_0}+b\left[\frac{\rho(\mathbf{r})}{\rho_0}\right]^{1+\nu}\ . \tag{2.3}$$

This oversimplified effective force reproduces the basic properties of finite nuclear matter such as saturation density and ground-state binding energies. However, it has no explicit or implicit momentum dependence (the effective mass is unity); then it fails in reproducing the energy dependence of the optical potential depth. The only degree of freedom of this effective force is the nuclear incompressibility modulus K_∞; when using the Zamick force in a wide beam energy range, the needed adjustment leads to a spurious sensitivity of the results with respect to K_∞.

To illustrate the influence of K_∞ on the collision dynamics, the two sets of parameters that have been used are presented in Table I.

On the other hand, in this work, we also shall use extensively the Gogny force [9], which is nonlocal. It reproduces many nuclear properties [9], in particular, the optical potential depth and Landau parameters (quantities which have not been used to adjust the parameters of the force). In the phase space representation, the corresponding mean-field potential without spin-orbit term reads

$$V_{\text{HF}}(\mathbf{r},\mathbf{p})=\tfrac{7}{8}t_3\rho^{4/3}(\mathbf{r})+\sum_{i=1}^{2}\alpha_i\int d^3r'\,e^{-(\mathbf{r}-\mathbf{r}')^2/\mu_i^2}\rho(\mathbf{r}')$$
$$-\sum_{i=1}^{2}\beta_i\int d\mathbf{p}'\,e^{-(\mu_i^2/4\hbar^2)(\mathbf{p}-\mathbf{p}')^2}f(\mathbf{r},\mathbf{p}')\ , \tag{2.4}$$

with

$$\alpha_i=W_i+\frac{B_i}{2}-\frac{H_i}{2}-\frac{M_i}{4}\ , \tag{2.5a}$$

$$\beta_i=\left[\frac{W_i}{4}+\frac{B_i}{2}-\frac{H_i}{2}-M_i\right](\sqrt{\pi}\mu_i)^3\ . \tag{2.5b}$$

In this representation the mean field exhibits space and momentum dependences; the resulting effective mass is then comparable to the microscopically calculated one only on the average; the effective mass enhancement close to the Fermi energy is not reproduced, since genuine energy-dependent processes are ignored.

The functional form of the Gogny force is well adapted to describe analytically the mean field in terms of Gaussians. This force has been adjusted to ground-state properties of nuclei and should be trustworthy up to momentum transfers of at least the order of the Fermi momentum. It has been shown [6] to reproduce well the energy dependence of the real part of the optical potential up to $\approx$200 MeV.

The standard parameters of the Gogny force are given in Table II; the resulting effective mass is $m^*/m=0.67$, and the incompressibility modulus is $K_\infty=228$ MeV. This latter parameter is not well settled, recent experimental analyses [10] suggesting higher values; however, their fit is far from unique (see, for example, Ref. [11]); and recent calculations with generalized Skyrme-type interactions indicate that $170<K_\infty<200$ MeV [12]. We shall use here other parameters sets, yielding different K_∞ values while preserving most of the other properties of the Gogny force. However, the fulfillment of the sum rules of the Landau parameters and of good pairing properties has to be relaxed. Let us just mention that the present model generates a well defined mean field with a proper surface dependence and includes the Coulomb force, which is essential to transverse motions at low energies.

The collision term of Eq. (2.1) is simulated by the collisions between coherent states, which are considered as hard test particles. The procedure has been successfully

TABLE I. Zamick interactions parameters.

Zamick Interaction	a	b	ν	K_∞	m^*/m
Soft	−356	303	1/6	200	1
Stiff	−123	70	1	380	1

TABLE II. Gogny interaction G1-D1 parameters.

Gogny Interaction	i	μ_i	W_i	B_i
D1-G1	1	0.7	−402.40	−100.00
	2	1.2	−21.30	−11.77
Gogny Interaction	H_i	M_i	t_3	
D1-G1	−496.20	−22.36	1350	
	−32.27	−68.81	1350	

checked by comparisons with analytical results of solvable models [13]. The nucleon-nucleon cross section, isospin, and energy dependence are corrected for in-medium effects according to the Brueckner calculations of Ref. [14]; the resulting effective σ_{nn} in comparison with the free one is reduced.

III. ANALYSIS OF EXPERIMENTAL RESULTS

A. Transverse momentum analysis

Since experimental evidence [15–23] of transverse collective motion is currently available for incident energies per nucleon below 100 MeV, we now turn to a quite detailed comparison with the experimental data. This comparison will permit us to check if our model allows quantitative confrontation with experiments and if it can provide reliable information on possible signatures either of the nuclear EOS or residual interactions. However, as stated before, our theoretical approach describes the overall dynamics in terms of one-body distribution functions, and then it should only be relevant for observables not affected by fragment formation. Other works are in progress to take this into account, but they are beyond the scope of this paper.

The most common way to single out transverse collective motion either at high [24–28] or low [15–23] energies is to analyze the mean transverse momentum in the reaction plane as a function of the longitudinal rapidity, according to the so-called transverse momentum analysis [7]. We will apply this method and discuss the different filters which have to be introduced in order to lead to meaningful comparisons between theoretical and experimental results. Our investigation is connected with recent experiments [20–23] performed at GANIL with Ar+Al system for incident energies ranging from 45 to 85 MeV/nucleon. These inverse kinematic reactions of an asymmetric system appear to provide an efficient way [23] to select the impact parameter. We will analyze semicentral collisions with an impact parameter of 3 fm.

In Fig. 1 we have plotted the mean transverse momentum as a function of the longitudinal rapidity. The circles correspond to the results obtained for the total system. Our first step will be to simulate the detector acceptance. According to Ref. [23], a first model of this acceptance consists in removing the nucleonic distributions having velocities in the laboratory lower than $0.1c$. In Fig. 1 this procedure has been called "filter 1" and the corresponding results are given by solid squares when they differ from those of the total system (circles). We note that significant differences appear only below and around $Y_z = 0.1$. The main consequence is the increase of the apparent transverse momentum at low rapidity, since nucleons with low transverse and longitudinal momenta are not taken into account. This filter is only efficient for an incident energy of 45 MeV/nucleon, and in consequence it has not been plotted for the 65 MeV/nucleon incident energy. A second fit of the detector acceptance has also been introduced, removing all the nucleonic distribution with velocities below 0.2 times the light velocity. This second estimation, called "filter 2," has been chosen because of the increase of the detection velocity threshold with the mass of the detected fragments. In Fig. 1 the corresponding results are plotted with solid circles when they differ from those of the total system (open circles). For the two incident energies considered here, this filter has important effects on the mean transverse momentum at low longitudinal rapidities. Therefore, in this range of energy, we expect a quite strong increase of the apparent transverse momentum with the fragment mass for Y_z below the center-of-mass rapidity $Y_{\text{c.m.}}$. Let us just note that in our one-body description the second filter is certainly too drastic. Nevertheless, we have chosen to display the results provided by the two previ-

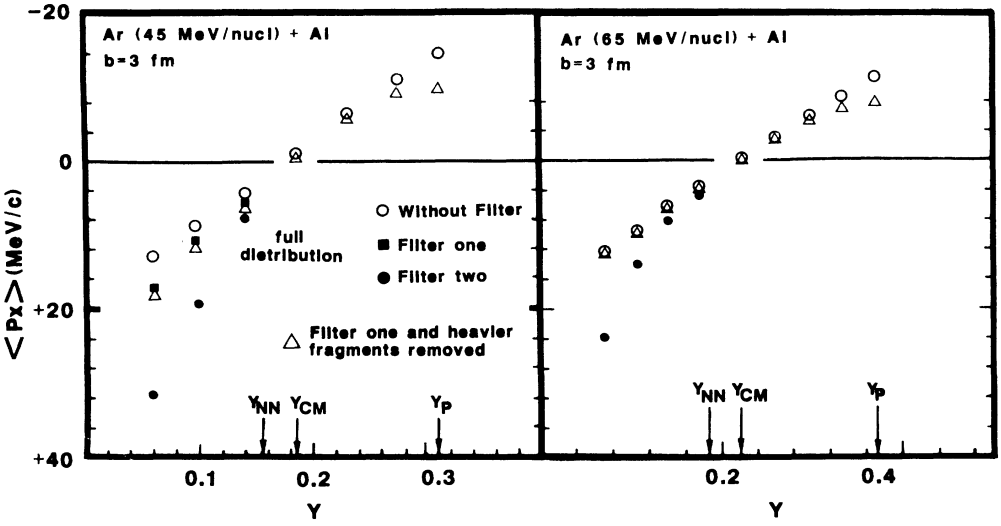

FIG. 1. Mean transverse momentum in the reaction plane as a function of the longitudinal rapidity. The effects of various experimental filters are theoretically simulated (see text for details). The arrows indicate, on the abscissas, the rapidities of the projectile y_p the center-of-mass $y_{\text{c.m.}}$, and the nucleon-nucleon frame y_{nn}. Note the reversed scale of the flow chosen for comparison with experimental data.

ously defined filters in order to give quantitative information on the variation of the apparent transverse momentum with the detection velocity threshold.

The experimental results describe the transverse motion of fragments with a charge up to 2 units. Therefore we have plotted with triangles the theoretical mean transverse momentum removing the heavier fragments from the total system and using filter 1. In the low rapidity domain, there are no significant modifications, since filter 1 already cancels the contributions of possible residues from the target. On the contrary, at high longitudinal rapidities, a decrease of the transverse momentum can be observed. This shows that the residue of the projectile experiences a more pronounced negative deflection, since it is essentially affected by the attractive character of the nuclear interaction and is practically insensitive to the compression in the entrance phase of the collision.

For reliable comparisons with experimental data, an additional step is still needed. In experiments a finite number of charged particles is detected, inducing an undetermination on the estimate of the reaction plane over which the mean transverse momentum is calculated. To take into account this fundamental effect in the Landau-Vlasov model, according to Ref. [28], each element of the initial coherent state basis has been considered as a nucleonic degree of freedom, and the finite number effect is analyzed from a statistical point of view, associating at random a coherent state to each nucleon of the final distribution. Then each random selection in the statistical ensemble represents an event.

In agreement with the experimental procedure given in Ref. [23], the reaction plane is defined for each particle i in each event by the beam axis direction and vector:

$$\mathbf{Q}_i = \sum_{\substack{j=1 \\ j\neq i}} w_j(\mathbf{p}_j^{\perp} + m_j \mathbf{V}_i^{(b)}) , \tag{3.1}$$

where $\mathbf{p}_j^{\perp}$ is the transverse momentum of the particle j and $w_j = y_j - y_{\text{c.m.}}$, y_i and $y_{\text{c.m.}}$ being, respectively, the particle j and the center-of-mass rapidities. Consistently with the prescription of Ref. [16], a recoil velocity correction was introduced with the velocity:

$$\mathbf{V}_i^b = \frac{\mathbf{p}_i^{\perp}}{m_{\text{sys}} - m_i} , \tag{3.2}$$

where m_{sys} is the sum of the masses of the projectile and target. In addition, for a better fitting of the experimental efficiency [22], a random selection of the detected nucleons was assumed in order to obtain a linear momentum of about 70% of the projectile initial momentum. It must be stressed that a genuine simulation of the experimental conditions should require a proper description of all detected particles (clusters, fragments), the error on the reaction plane increasing with the particle mass. Let us note that the theoretical estimate of the reaction plane indetermination is very close to the experimental one [23]. This is due to the incomplete paving of the nuclei initial phase space together with fluctuations induced by the simulation of the residual interactions.

The corrected results of the Landau-Vlasov model for the emitted particles without the heavier fragments, taking into account both the detector acceptance with the first filter and the reaction plane indetermination, are plotted in Fig. 2 in comparison with experimental results. First, let us note that the corrected theoretical results shown as open circles exhibit similar shapes to the experimental ones: a plateau near the initial projectile rapidity and a quasilinear behavior at lower rapidities due to the filter introduced to simulate the detectors acceptance. In the lower rapidity region, the detection threshold having less influence with increasing energy, our theoretical results tend to reach intermediate values between those displayed for $Z=1$ and 2. This is consistent with the fact that our approach is essentially a one-body description, where higher order correlations are dropped. Being unable to discriminate individual nucleons from those be-

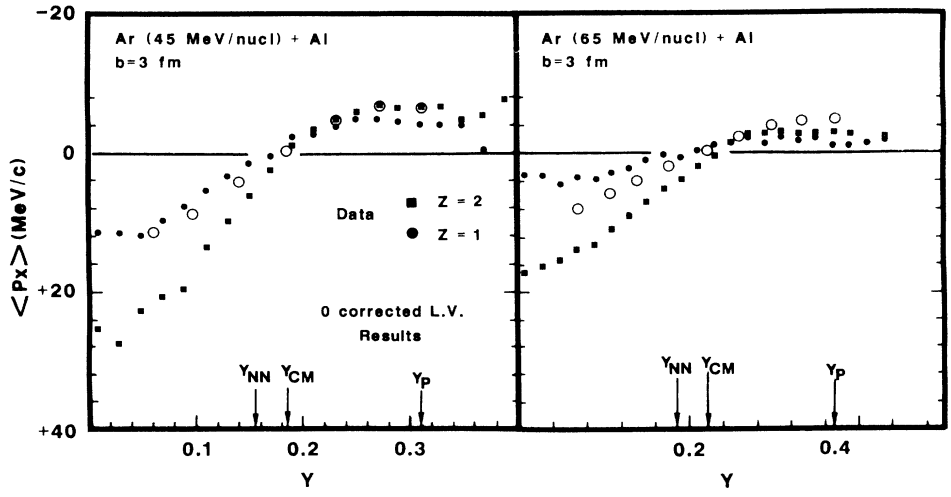

FIG. 2. Mean transverse momentum in the reaction plane as a function of the longitudinal rapidity. The solid squares and circles show the experimental [23] results for $Z=1$ and 2 fragments. The theoretical results, shown by open circles, are corrected for the detector efficiencies and reaction plane indetermination.

longing to clusters, we are only allowed to give the overall $\langle p_x \rangle$ distribution, which provides intermediate values between those corresponding to fragments. The multiplicity of heavy clusters is a growing function of incident energy; their weight is expected to be weaker at low energy. This aspect can be observed in Fig. 2, where a rather good agreement of $Z=1$ values with the theoretical ones is found for $E=45$ MeV/nucleon. The $Z=1$ and 2 experimental results present net different values in the low rapidity domain. Nevertheless, a conspicuous dependence of the transverse momentum on the fragment mass arises. This effect can be connected with a similar trend appearing at higher energies [30]. However, in this latter case, this can be related to the repulsive action provided by a highly compressed nuclear matter, whereas in the energy domain we are interested in, the negative deflection increases with the fragment mass, showing a greater sensitivity to the attractive component of the nuclear interaction.

In the higher rapidity region, a weak fragment mass dependence still remains. Our theoretical results overestimate slightly the experimental data. Tentative explanations can be advanced. First, in the corrected theoretical results, only the heavy fragments have been removed, and our one-body distribution could include $Z>2$ fragment mass, which contributes with slightly greater transverse momenta. Second, the experimental results displayed in Fig. 2 do not include the recoil velocity correction, which accounts for the total momentum conservation. According to Ref. [23], this leads to a weakening of the absolute $\langle p_x \rangle$ experimental values in the higher rapidity domain and this effect increases with impact parameter and low flows.

B. Flow observable around the energy of vanishing flow

According to Ref. [7], let us define the flow observable as

$$\mathcal{F}=\left.\frac{\partial\langle p_x \rangle}{\partial y_z}\right|_{\tilde{y}_x=0}, \tag{3.3}$$

where $\tilde{y}_z=y_z/y_{\text{proj}}$ is the rapidity normalized to the projectile rapidity and $\langle p_x \rangle$ is the mean transverse momentum projected on the reaction plane and is given by

$$\langle p_x \rangle=\frac{\int d^3r\, dp_x\, dp_y\, p_x f(\mathbf{r},\mathbf{p})}{\int d^3r\, dp_x\, dp_y\, f(\mathbf{r},\mathbf{p})} . \tag{3.4}$$

Then the flow is merely the slope of the curves displayed in Fig. 2 at the center-of-mass rapidity $Y_{\text{c.m.}}$. It essentially characterizes the momentum transfer from longitudinal to transverse components in the participant region. Roughly speaking, the collective flow is usually interpreted as the result of two opposite dynamical effects: the attractive mean field, which tends to deflect fragments to negative scattering angles, and the repulsive internal pressure created mainly in the entrance channel of the collisions by the residual interactions and nuclear matter compression. For a given system of colliding nuclei, the relative weight of both dynamical contributions obviously depends on the incident energy, mass, and impact parameter and determines the sign of the flow.

It is currently well established from experiments [15–23] that for beam energies below 150 MeV/nucleon the flow observable evidences net transverse collective motions of nuclear matter, but apart from a narrow region of beam energies, where it vanishes. As already mentioned, we will call this region the energy of vanishing flow (EVF). Even if most experiments cannot discriminate between positive and negative deflections, the flow behavior clearly indicates a transition in the collective motion with a flow inversion. At variance with the flow observable, the EVF is practically insensitive to experimental biases and corrections are useless since we deal with zero values. In addition, experiments seem to reveal no (or at least) weak sensitivity of the EVF on the detected fragment masses. Consequently, we will not introduce in this section the corrections previously discussed and the following theoretical flows will be given uncorrected.

In Fig. 3 theoretical flow values are plotted versus energy for the Nb+Nb, Ca+Ca, and C+C systems, keeping nearly constant the ratio of the impact parameter to the linear dimension. This constraint aims at preventing the relative weight of mean field and collision term to change due to geometrical scalings. The EVF values are indicated by arrows. A clear increase of this quantity is observed for decreasing masses, following approximately an $A^{-1/3}$ law, consistent with the fact that the rate of two-body collisions is a growing function of A.

This mass dependence results from a complicated mixture of one- and two-body effects; a rough interpretation can be tentatively advanced from a hydrodynamical point of view. For a discussion of scaling properties of heavy-ion reactions in a hydrodynamic model, see Ref. [31]. In this picture the collective motion pattern is completely

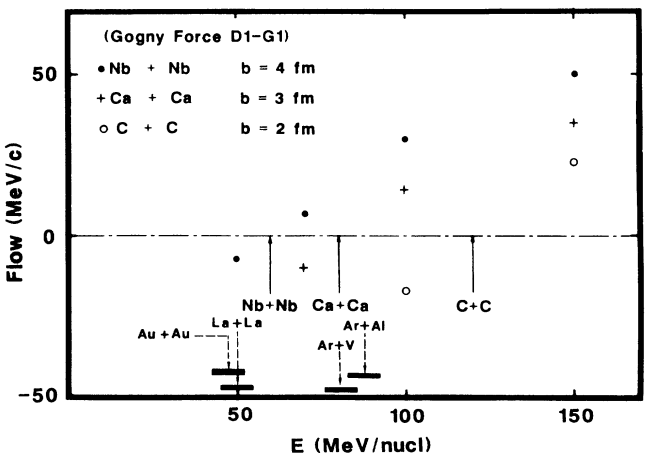

FIG. 3. Collective sideward flow, calculated with the Gogny D1-G1 force, as a function of incident energy per nucleon, for three different symmetric systems. Experimental estimates of the energy of vanishing flow are also indicated: La+La [14], Ar+V [17], Ar+Al [23], and Au [19]. In the lower part of the figure, the horizontal bars give the experimental uncertainties.

determined by the Reynolds number $\mathrm{Re}=ul/\nu$, where u represents the incident velocity, l is the characteristic linear dimension of the system, and ν is the kinetic viscosity. This latter quantity has been already estimated in the framework of the Uehling-Uhlenbeck collision term [32]. Nevertheless, in a first approximation, it is proportional to both u and the mean free path λ, whose behavior, in the energy range we are interested in, is roughly inversely proportional to the incident energy E. Consequently, the Reynolds number scales as $EA^{1/3}$, where A is the mass number of the system. Assuming that at the EVF the Reynolds number is the same for all systems, we obtain a $A^{-1/3}$ mass number law for the energy. For sake of comparison, we have also indicated some experimentally estimated EVF's on the abscissa of Fig. 3. Although the experimental errors are quite large, we observe that the mean values are in good agreement with the theoretical predictions.

Experimental data for the flow under the EVF show clear dependence on the fragment masses. Our model cannot describe cluster formation; however, it can give indications on the role of the Coulomb repulsion. In Fig. 4 we show the dependence of the flow on the Coulomb interaction. The solid squares and circles are the flow estimated [23] from the primary experimental measurements, respectively, for the $Z=1$ and 2 fragments. We have also plotted the theoretical flow observables not corrected from the experimental inefficiency since we are dealing with qualitative trends. In Fig. 4 the triangles, circles, and squares are, respectively, associated with the nucleon, neutron, and proton flows. We observe a clear isospin dependence of the flow, likely due to the Coulomb repulsion, which induces weaker negative deflections for the protons. To check this we have suppressed the Coulomb interaction in the model, and then the associated flow appears to be close to the one found with by the neutrons alone. Consequently, a partial understanding of the particle charge dependence of the collective transverse motion can be assigned to the Coulomb repulsion in this low energy domain, since $Z=1$ particles are mainly protons and $Z=2$ particles are composites. The increasing weight of the neutrons induces greater negative deflection.

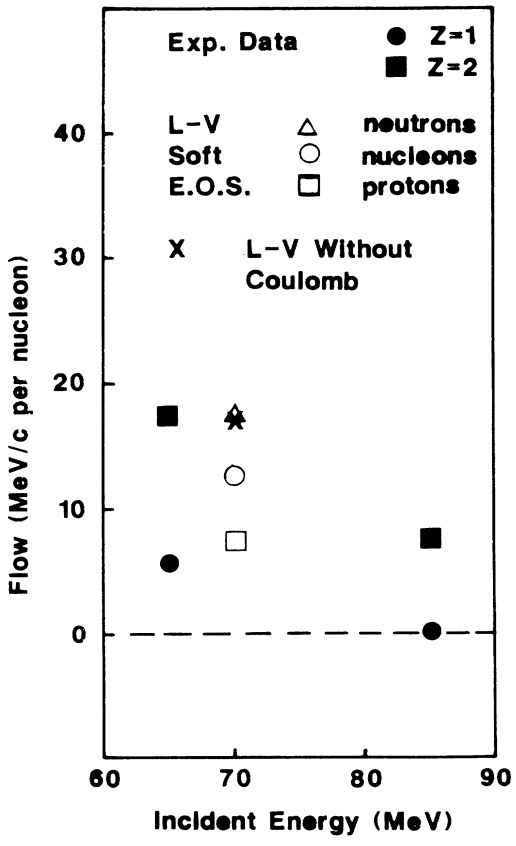

FIG. 4. Effects of the Coulomb repulsion on the absolute value of the theoretical flow for Ar+Al system. Experimental values [24] are also indicated for the same system.

IV. FLOW OBSERVABLE SENSITIVITY TO NUCLEAR MATTER PROPERTIES

The Landau-Vlasov description was shown to be in good agreement with the experimental flow measurements. The question which arises now is what kind of information can we extract from it. In other words, can a semiclassical approach to heavy-ion dynamics teach us something new on nuclear matter properties through a flow analysis? In order to clarify this question, we study in this section the dependence of the flow observable on the nucleon-nucleon cross section and on the parameters of a realistic effective force given by the finite range Gogny force presented in Sec. II. In Fig. 3 a clear mass number dependence of the EVF was observed. It shows that nucleon-nucleon collisions are of growing importance as A increases. Indeed, the number of individual nucleon-nucleon collisions diminishes very rapidly for lighter nuclei, whereas the mean field stays rather well defined. As a consequence, we can expect to find also an important dependence of the EVF on σ_{nn}.

In Fig. 5 some typical values of the flow as a function of the incident energy for the Ca+Ca system are shown. The in-medium corrected [14] nucleon-nucleon cross section entering in the collision term is slightly scaled up and down. We observe that a 20% variation of σ_{nn} induces a shift of roughly 10 MeV/nucleon on the EVF. Current improvements of experimental accuracy should provide valuable information on that point, since a weak dependence of the EVF on the mean-field parameters is expected [2]. Let us note that our results are in approximate agreement with a recent investigation by Olgivie *et al.* [18], but one must take into account that in that reference the free nucleon-nucleon cross section was used while our in-medium corrected one is roughly 50% smaller. From Fig. 5 we also note that a slight scaling of σ_{nn} leaves the slope of the flow near the EVF practically unaltered, whereas this latter quantity could be more sensitive to the EOS, as far as local mean fields are concerned [2].

In heavy-ion collisions at energies above the EVF, flow calculations [1] exhibit a strong dependence on the incompressibility modulus K_∞ for local forces. The intro-

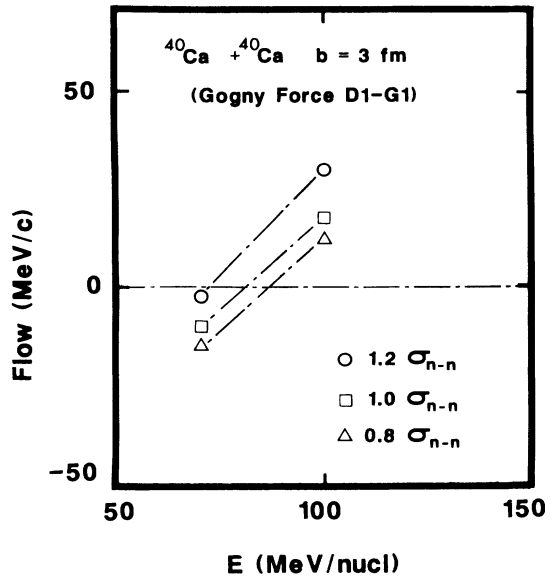

FIG. 5. Collective sideward flow as a function of incident energy per nucleon, for the Ca+Ca system at an impact parameter of 3 fm and for different scalings of the nucleon-nucleon cross section.

duction of momentum-dependent terms in the interactions has been shown to increase notably the collective flow for a given value of K_∞. Whether unambiguous signatures of the EOS can be extracted from the flow when it is calculated with nonlocal forces still remains an unanswered question. To gain more insight on that point, we made calculations using a set of Gogny D1-type interactions with different values of K_∞ and effective mass m^*/m. Basic infinite nuclear matter properties such as the saturation density and binding energy per nucleon were kept at the D1 values. In addition, the ranges of our forces are the same as in D1. For all those interactions we checked that the stability conditions established by Migdal [33] were met. Nevertheless, the sum rule constraints and good pairing properties were released in order to investigate ranges of K_∞ and m^* values as large as possible. In the self-consistent treatment of the Landau-Vlasov static solution, it has been checked that the set of parameters considered provides good ground-state properties of finite nuclei such as binding energies and mean square radii.

Since the mean-field contribution to the buildup of transverse collective motion is based on its momentum dependence as well as on its density dependence, let us now briefly outline how they show up in K_∞ and m^* via characteristic parameters of the nuclear interactions. The effective mass is directly connected with the momentum dependence as it stems from its definition:

$$m/m^* = \frac{m}{\hbar^2}\frac{1}{k_F}\left[\frac{d}{dk}\varepsilon(k)\right]_{k=k_F}, \tag{4.1}$$

where $\varepsilon(k)$ is the one-particle energy in infinite nuclear matter and k_F the Fermi wave number. For our finite range interactions, we have the following expression for m/m^*:

$$m/m^* = \frac{m}{\hbar^2}\frac{k_F}{2\sqrt{\pi}}\sum_{i=1}^{2} g_i \mu_i^3 e^{-x_i}\left[\frac{\cosh(x_i)}{x_i} - \frac{\sinh(x_i)}{x_i^2}\right], \tag{4.2}$$

where

$$g_i = W_i + 2(B_i - H_i) - 4M_i \tag{4.3a}$$

and

$$x_i = \frac{k_F^2 \mu_i^2}{2}, \tag{4.3b}$$

the previous coefficients W_i, B_i, H_i, M_i, and μ_i being defined in Table II for the D1-G1 parametrization. A convenient and good estimate of the K_∞ parameter can be made within the effective mass approximation [34] for finite range forces of Gogny D1 type whose momentum dependence is completely included in the Fock contribution of the mean field. In this approximation the nonlocal exchange term is evaluated using a momentum expansion up to second order:

$$u^{\text{exc}}(k) \simeq u^{\text{exc}}(k=0) + a^{\text{exc}} k^2 . \tag{4.4}$$

This allows one to write the infinite compressibility modulus K_∞ in the form

$$K_\infty = \frac{3}{5}\frac{\hbar^2}{m}k_F^2\left[2\left[\frac{m}{m^*}\right] - 3 + 3\rho_\infty\left[\frac{m}{m^*}\right]'_{\rho_\infty}\right] + \frac{27}{8}t_3\gamma(\gamma+1)\rho^{\gamma+1}, \tag{4.5}$$

where $(m/m^*)'$ is the derivative of (m/m^*) with respect to the density ρ. The last term of Eq. (4.5) arises from the density-dependent part of the Gogny force. The K_∞ expression can be put in a simpler form for Skyrme-type forces; it then reads

$$K_\infty = \frac{3}{5}\frac{\hbar^2}{m}k_F^2\left[5\left[\frac{m}{m^*}\right] - 6\right] + \frac{27}{8}t_3\gamma(\gamma+1)\rho^{\gamma+1} . \tag{4.6}$$

Although Eq. (4.6) is not exact for finite range forces, it is still a good approximation to the exact K_∞; moreover, it has the advantage of showing in a clear way that the main contribution to K_∞ comes from the density-dependent part of the interaction. However, the latter significantly weakens with decreasing effective mass.

In Fig. 6 we have visualized separately the effect of K_∞ and m^* on the flow created by a symmetric system in a semicentral collision with an incident energy of 100 MeV per nucleon. In agreement with theoretical calculations performed at higher energies [35], we note the flow enhancement with decreasing effective masses. The expected trend stems from the fact that smaller m^*/m result from stronger momentum gradients of the mean field, generating stronger flow. A less expected behavior is the insensitivity of the flow observable on K_∞ for lower m^*/m. In a discussion of Eq. (4.6), it has been stressed that the weight of the density-dependent contribution in K_∞ decreases with the effective mass. It should still pro-

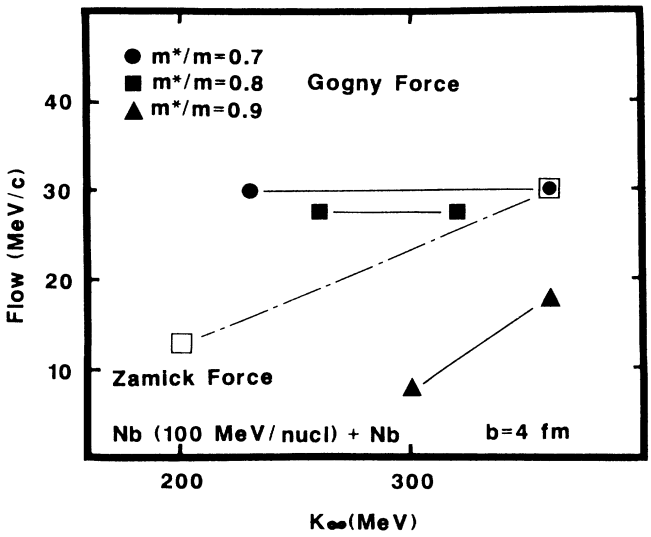

FIG. 6. Flow values calculated with the Gogny force for various incompressibility moduli and average effective masses.

vide an enhancement of the flow, though weaker. However, the previous arguments are only founded on static considerations. Only the dynamical mechanism of the flow buildup can explain this behavior. As a matter of fact, two effects cooperate to wash out the K_∞ signatures. First, decreasing effective masses leads to greater velocities of the nucleon in nuclear matter, including greater spreading and lower densities. Second, as already pointed out in other works [2], the momentum dependence of the mean field acts more efficiently at the very beginning of the collision, when the nucleon relative velocities of the colliding nuclei are large and before densities higher than the saturation one occur in the interacting area.

In order to shed light on the flow dependence on the various Gogny forces, we have drawn in Fig. 7 the real part of the nonlocal optical potential as a function of the energy for some characteristic cases. It clearly appears that similar energy dependences above the Fermi energy generate practically the same flow values, even if the effective mass values (determined at the Fermi level) are different. It can be also observed in Fig. 6 that the K_∞ dependence of the Zamick forces is recovered, constraining the Gogny force to be almost local ($m^*/m=0.9$). In this case the energy dependence of the mean field does not agree with experimental data, as is pointed out in Fig. 7. The tight connection between flow values and the momentum dependence of the mean field underlines the fundamental role played by nonlocality effects in the dynamical creation of transverse collection motion.

The insensitivity of the flow on the incompressibility modulus for the various Gogny-type forces may seem deceiving. One should bear in mind, however, that in order to do so we had to relax a certain number of important constraints (see above). It does not at all seem evident to find Gogny-type forces which fulfill all requirements of the original one and which solely have the incompressibility modulus changed. Although one cannot exclude with rigor that such a force exists, we have concluded that the good agreement of calculated flow data with experiment does not provide any reason to change the value $K=228$ MeV obtained from the D1 force.

As previously mentioned, the transverse collective motion in heavy-ion collisions bears signatures of nuclear matter properties. We will now give a better understanding of what kind of information could be extracted and what part of the nuclear EOS is explored. To illustrate these points we consider a semicentral collision of a symmetric system with an incident energy of 150 MeV per nucleon in the laboratory frame. Although this incident energy is above the energy range we are dealing with, it provides the advantage of clearly exhibiting the general trends we are interested in. Therefore some typical trajectories of the colliding system in the EOS have been investigated from different effective interactions.

To provide a close connection with what is commonly referred to as the nuclear EOS, we display in Fig. 8(a) the average cold energy density per nucleon in the interacting zone of the colliding system as a function of the nuclear matter density achieved in this region. To define precisely our estimate of this cold energy density per nucleon, let us start from the energy density $\varepsilon(\mathbf{r})$:

$$\varepsilon(\mathbf{r})=\tau(\mathbf{r})+\varepsilon_{\text{pot}}(\mathbf{r}) , \tag{4.7}$$

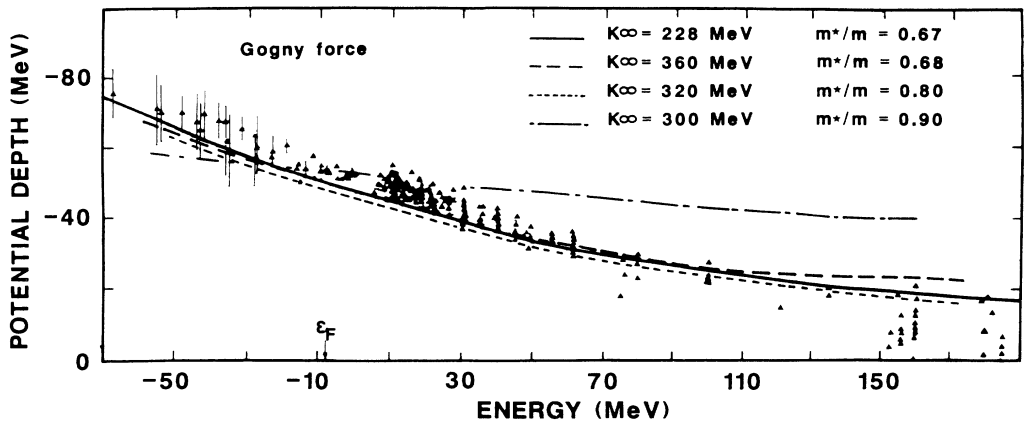

FIG. 7. Behavior of the potential depth for some Gogny-type forces.

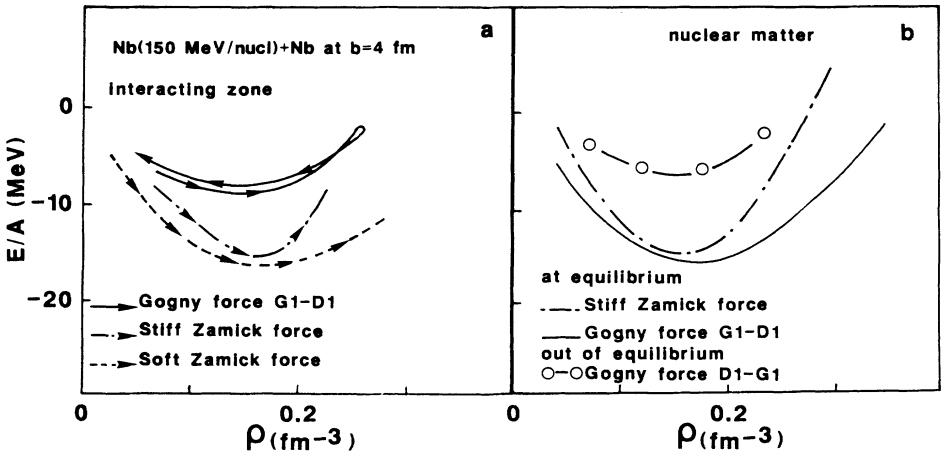

FIG. 8. Static and dynamic behaviors of the equation of state for local and nonlocal forces. (a) Dynamical trajectories occurring in the interacting zone of a colliding system. (b) Infinite nuclear matter calculations either at equilibrium or out of equilibrium (see text for details).

where $\tau(\mathbf{r})$ is the kinetic energy density and $\varepsilon_{\text{pot}}(\mathbf{r})$ the potential energy density obtained by a functional integral of the one-body Hartree-Fock potential. The kinetic energy density can be split into collective and intrinsic contributions:

$$\tau(\mathbf{r})=\tau_{\text{coll}}(\mathbf{r})+\tau_{\text{int}}(\mathbf{r}) , \tag{4.8}$$

with a collective kinetic energy density defined by

$$\tau_{\text{coll}}(\mathbf{r})=\tfrac{1}{2}m\rho(\mathbf{r})u^2(\mathbf{r}) , \tag{4.9}$$

where $\rho(\mathbf{r})$ is the local matter density and $\mathbf{u}(\mathbf{r})$ the local collective velocity, which reads

$$\mathbf{u}(\mathbf{r})=\frac{1}{\rho(\mathbf{r})}\int\frac{\mathbf{p}}{m}f(\mathbf{r},\mathbf{p})d\mathbf{p} . \tag{4.10}$$

The definition of the intrinsic kinetic energy density allows one to separate it into two contributions:

$$\tau_{\text{int}}(\mathbf{r})=\tau^*(\mathbf{r})+\tau_{\text{TF}}(\mathbf{r}) , \tag{4.11}$$

where $\tau_{\text{TF}}(\mathbf{r})$ is a Thomas-Fermi approximation of the cold kinetic energy density and the remainder $\tau^*(\mathbf{r})$ is called the excitation energy density. More accurately, the numerical evaluation of the local cold kinetic energy density in the Thomas-Fermi approximation stems from an iterative procedure in which a sharp Fermi bisphere representation in momentum space has been used, fitting its characteristic parameters (namely, the excentricity and radius) to the local matter density and to the quadrupole moment of the momentum distribution. Consequently, we have defined the cold energy density per nucleon by

$$w(\mathbf{r})=\frac{\tau_{\text{TF}}(\mathbf{r})+\varepsilon_{\text{pot}}(\mathbf{r})}{\rho(\mathbf{r})} . \tag{4.12}$$

We observe in Fig. 8(a) that the dynamical trajectories related to local forces follow closely the behavior imposed by the nuclear EOS of corresponding K_∞, drawn in Fig. 8(b). When nonlocal effects are taken into account, for example, with the Gogny force, the dynamical trajectory exhibited in Fig. 8(a) clearly differs from the cold nuclear EOS at equilibrium. However, this trajectory is directly connected to infinite nuclear matter properties. To check this point, calculations at different densities have been performed with two pieces of cold nuclear matter in relative motion one against the other. The out-of-equilibrium behavior has been adjusted to the evolution of the quadrupole momentum evolution in momentum space, and the related results are displayed by open circles in Fig. 8(b). We can remark that the dynamical trajectory of a nonlocal force follows closely the behavior of infinite nuclear matter when out-of-equilibrium effects are taken into account.

Beyond the determination of the infinite incompressibility modulus of cold nuclear matter at equilibrium, the transverse collective motion provides a convenient way to investigate out-of-equilibrium nuclear matter properties. In connection with current improvement of experimental data accuracy, study of energy, mass, and impact parameter dependences of collective phenomena should lead to more trusty evaluations of nuclear matter characteristic parameters, through confrontations with theoretical approaches, provided that they refer to realistic nuclear interactions.

V. CONCLUSIONS

In this work we performed a study of transverse collective motion in nuclear collisions at beam energies below 100 MeV/nucleon with the Landau-Vlasov model. In order to compare our theoretical results with experiment, the incomplete fragment detection of real measurement as well as detector efficiency has been numerically simulated and their influence in the final results discussed in detail. We showed that even though our microscopic one-body description does not account for fragment formation, it reproduces well the global trends of experimental results, both qualitatively and quantitatively. This comparison allowed us to find a net dependence of the en-

ergy of vanishing flow (EVF) with the mass number ($\sim A^{-1/3}$). Moreover, a strong sensitivity of the EVF to small variations of the nucleon-nucleon cross section was shown.

The calculations of flow values with different parametrization of the effective Gogny force point out a weak K_∞ dependence for low effective masses. The theoretical analysis shows the fundamental role played by the nonlocal component of the interaction and the crucial importance of dynamical and out-of-equilibrium effects in the creation of collective transverse motion.

As already stated in different works, the flow observable should be a convenient probe of nuclear matter properties, since (1) it is mostly determined in the overlapping region where the closest conditions to the nuclear matter are reached, (2) it is created in the early stage of the reaction where the higher densities and relative momenta are achieved, and (3) it survives the expansion stage of the reaction. Our semiclassical approach with a realistic effective interaction underlines that this observable cannot give direct information on the magnitude of the incompressibility modulus of cold nuclear matter at equilibrium.

This stems mainly from the fact that the flow is built up in the early stage of the reaction where one essentially has two interpenetrating pieces of nuclear matter rather than one hot and compressed but equilibrated interaction zone. In the determination of the flow, the energy dependence of the mean field is then of prime importance. Indeed, we showed in this paper using various Gogny type of forces that as long as this energy dependence is such as to reproduce the experimental data the flow is insensitive to the incompressibility modulus. This may find its explanation in the relatively weaker compression of the interaction zone for nonlocal mean fields compared with local ones such as, e.g., the Zamick forces. The decreasing depth of the mean-field potential with energy seems therefore the main source for repulsion and therefore for the flow. One must mention, however, that our calculations with the Gogny force do reproduce the data and that it seems difficult to change its characteristics without giving up some of the important conditions the original force satisfies. From our point of view, the flow data do not give any firm reason to deviate from the canonical value $K_\infty = 210 \pm 30$ MeV [36].

We also must emphasize that the energy dependence of the mean field considered here stems only from the nonlocality of the force (k mass). For energies around the Fermi energy, which may play a role at the bombarding energies $E/A < 100$ MeV we are considering here, one has in addition to take into account a genuine energy dependence (E mass) of the mean field. Whether the incorporation of such refined effects will reinforce the sensitivity to the EOS remains to be seen.

[1] H. Stöcker, in Proceedings of the International Conference on Nuclear Matter and Heavy-Ion Collisions, les Houches, 1989 (unpublished).

[2] V. De La Mota, F. Sébille, B. Remaud, and P. Schuck, LPN report, 1990 (unpublished); in Proceedings of the XXVII Winter Meeting on Nuclear Physics, Bormio, Italy, 1990 (unpublished).

[3] G. F. Bertsch, W. G. Lynch, and M. B. Tsang, Phys. Lett. B **189**, 384 (1987); A. Bonasera and L. P. Csernai, Phys. Rev. Lett. **59**, 630 (1987); H. M. Xu, *ibid.* **67**, 2769 (1991).

[4] E. Suraud, M. Pi, P. Schuck, B. Remaud, F. Sébille, C. Grégoire, and F. Saint Laurent, Phys. Lett. B **229**, 359 (1989).

[5] C. Grégoire, B. Remaud, F. Sébille, L. Vinet, and Y. Raffray, Nucl. Phys. **A485**, 317 (1987).

[6] F. Sébille, G. Royer, C. Grégoire, B. Remaud, and P. Schuck, Nucl. Phys. **A501**, 137 (1989).

[7] P. Danielewicz and G. Odyniec, Phys. Lett. B **157**, 146 (1985); P. Danielewicz *et al.*, Phys. Rev. C **38**, 120 (1989).

[8] J. Jiang, D. Keane, J. Cogar, G. Fai, S. Hayashi, C. Hartnack, and H. Stöcker, Phys. Rev. C **43**, 2353 (1991).

[9] J. Dechargé and D. Gogny, Phys. Rev. C **21**, 1568 (1980).

[10] M. M. Sharma, W. Stocker, P. Gleissl, and M. Brack, Nucl. Phys. **A504**, 337 (1989).

[11] J. M. Pearson, Phys. Lett. B **271**, 12 (1991).

[12] M. Farine (unpublished).

[13] G. Welke, R. Malfliet, C. Grégoire, M. Prakash, and E. Suraud, Phys. Rev. C **40**, 2611 (1989).

[14] J. Cugnon, A. Lejeune, and P. Grangé, Phys. Rev. C **35**, 861 (1987).

[15] D. Krofcheck *et al.*, Phys. Rev. Lett. **63**, 2028 (1989).

[16] C. A. Olgivie *et al.*, Phys. Rev. C **40**, 2592 (1989).

[17] C. A. Olgivie *et al.*, Phys. Lett. B **231**, 35 (1989).

[18] C. A. Olgivie *et al.*, Phys. Rev. C **42**, 10 (1990).

[19] W. H. Zhang *et al.*, Phys. Rev. C **42**, 491 (1990).

[20] J. Peter *et al.*, Phys. Lett. B **237**, 187 (1989).

[21] K. Hagel *et al.*, Phys. Lett. B **229**, 20 (1989).

[22] J. P. Sullivan *et al.*, Phys. Lett. B **249**, 10 (1990).

[23] J. Peter *et al.*, in Proceedings of the XXIX Winter Meeting on Nuclear Physics, Bormio, Italy, 1991 (unpublished); in Proceedings of the 4th International Conference on Nucleus Nucleus Collisions, Kanazawa, Japan, 1991 (unpublished).

[24] H. A. Gustaffson *et al.*, Phys. Rev. Lett. **52**, 1590 (1984).

[25] H. G. Ritter *et al.*, Nucl. Phys. **A447**, 3c (1985).

[26] K. G. R. Doss *et al.*, Phys. Rev. Lett. **57**, 302 (1986).

[27] M. Gutbrod, A. M. Poskanzer, and H. G. Ritter, Rep. Prog. Phys. **52**, 1267 (1989).

[28] K. H. Kampert, J. Phys. G **15**, 691 (1989).

[29] M. Zielinska-Pfabé and C. Grégoire, Phys. Rev. C **37**, 2594 (1989).

[30] J. W. Harris *et al.*, Nucl. Phys. **A471**, 241c (1987).

[31] N. L. Balazs, B. Schürman, K. Dietrich, and L. P. Csernai, Nucl. Phys. **A424**, 605 (1984).

[32] P. Danielewicz, Phys. Lett. **146B**, 168 (1984); A. Bonasera, L. P. Csernai, and B. Schürmann, Nucl. Phys. **A476**, 152 (1988).

[33] A. B. Migdal, *Theory of Finite Fermi Systems and Applications to Atomic Nuclei* (Interscience, New York, 1967).

[34] M. Farine, Ph.D. thesis, Université de Montreal, Montreal, 1981.

[35] W. Cassing and U. Mosel, Prog. Part. Nucl. Phys. **25**, 235 (1990).

[36] J. P. Blaizot, Phys. Rep. **64**, 171 (1980).